THE JOURNAL OF BIOLOGICAL CHEMISTRY VOL. 283, NO. 45, pp. 30503–30512, November 7, 2008

Apolipoprotein(a), through Its Strong Lysine-binding Site in KIV_{10}, Mediates Increased Endothelial Cell Contraction and Permeability via a Rho/Rho Kinase/MYPT1-dependent Pathway*

Received for publication, April 4, 2008, and in revised form, September 4, 2008 Published, JBC Papers in Press, September 5, 2008, DOI 10.1074/jbc.M802648200

Taewoo Cho, Yoojin Jung, and Marlys L. Koschinsky[1]

From the Department of Biochemistry, Queen's University, Kingston, Ontario K7L 3N6, Canada

Substantial evidence indicates that endothelial dysfunction plays a critical role in atherogenesis. We previously demonstrated that apolipoprotein(a) (apo(a); the distinguishing protein component of the atherothrombotic risk factor lipoprotein(a)) elicits rearrangement of the actin cytoskeleton in human umbilical vein endothelial cells, characterized by increased myosin light chain (MLC) phosphorylation via a Rho/Rho kinase-dependent signaling pathway. Apo(a) contains kringle (K)IV and KV domains similar to those in plasminogen: apo(a) contains 10 types of plasminogen KIV-like sequences, followed by sequences homologous to the plasminogen KV and protease domains. Several of the apo(a) kringles contain lysine-binding sites (LBS) that have been proposed to contribute to the pathogenicity of Lp(a). Here we demonstrate that apo(a)-induced endothelial barrier dysfunction is mediated via a Rho/Rho kinase-dependent signaling pathway that results in increased MYPT1 phosphorylation and hence decreased MLC phosphatase activity, thus leading to an increase in MLC phosphorylation, stress fiber formation, cell contraction, and permeability. In addition, studies using recombinant apo(a) variants indicated that these effects of apo(a) are dependent on sequences within the C-terminal half of the apo(a) molecule, specifically, the strong LBS in KIV_{10}. In parallel experiments, the apo(a)-induced effects were completely abolished by treatment of the cells with the lysine analogue ϵ-aminocaproic acid and the Rho kinase inhibitor Y27632. Taken together, our findings indicate that the strong LBS in apo(a) KIV_{10} mediates all of our observed effects of apo(a) on human umbilical vein endothelial cell barrier dysfunction. Studies are ongoing to further dissect the molecular basis of these findings.

Studies have shown that elevated concentrations of plasma lipoprotein(a) (Lp(a))[2] (>30 mg/dl or >100 nM) are a risk factor for a variety of vascular diseases, including coronary heart disease, ischemic stroke, and venous thrombosis (1, 2). Lp(a) is identical to low density lipoprotein (LDL) in both lipid composition as well as the presence of apolipoproteinB-100. However, Lp(a) is clearly distinguishable from LDL by the presence of the unique glycoprotein apolipoprotein(a) (apo(a)) that is disulfide-linked to apolipoproteinB-100 in LDL by a single disulfide bond (3). Apo(a) bears a striking homology with plasminogen and contains multiple repeats of a sequence that resembles plasminogen kringle IV as well as sequences homologous to the kringle V and protease regions of plasminogen (4). The protease domain in apo(a) cannot be activated by activators of plasminogen; therefore, it cannot develop protease activity and hence lacks fibrinolytic activity (5). The kingle IV-like domain in apo(a) is classified into 10 types (KIV_{1-10}); the KIV_2 sequence is present in a variable number of identically repeated copies (from 3 to >40) giving rise to Lp(a) isoform size heterogeneity (6, 7). Kringle IV types 5–8 (KIV_{5-8}) possess "weak" lysine-binding sites (LBS) (8) that mediate the non-covalent interactions between apo(a) and apolipoproteinB-100, which precede disulfide bond formation to form Lp(a). Another weak lysine-binding site is evident in kringle V (KV), and, as yet, its function is not known. Apo(a) also contains a "strong" LBS within kringle IV type 10 (KIV_{10}), which is thought to mediate binding of apo(a) and Lp(a) to other physiological ligands such as fibrin and extracellular matrix proteins (9, 10). Although many potential mechanisms by which Lp(a) might promote atherogenesis have been proposed (1, 2), the relevant mechanism(s) have yet to be definitively established. This uncertainty is likely a function of the complex, modular structure of apo(a).

The vascular endothelium forms a selective permeable barrier between the blood and the interstitial space of all organs and participates in the regulation of macromolecule transport and blood cell trafficking through the vessel wall. Failure of endothelial barrier function can occur when endothelial cells are exposed to inflammatory mediators, a key event in the initial stages of atherosclerosis. Loss of barrier function results from the opening of gaps between adjacent cells as a consequence of both a loss of cell adhesion and activation of the endothelial contractile machinery (11). Generation of contractile forces by endothelial cells (ECs) can cause adjacent cells to retract from each other (12, 13). The importance of this actin-myosin-based contractile apparatus for dynamic adaptation of

* This work was supported by the Heart and Stroke Foundation of Ontario (Grant T-5916 to M. L. K.). The costs of publication of this article were defrayed in part by the payment of page charges. This article must therefore be hereby marked "*advertisement*" in accordance with 18 U.S.C. Section 1734 solely to indicate this fact.

[1] A Career Investigator of the Heart and Stroke Foundation of Ontario. To whom correspondence should be addressed: Dept. of Biochemistry, Queen's University, A208 Botterell Hall, Kingston, Ontario K7L 3N6, Canada. Tel.: 613-533-6586; Fax: 613-533-2987; E-mail: mk11@queensu.ca.

[2] The abbreviations used are: Lp(a), lipoprotein(a); apo(a), apolipoprotein(a); r-apo(a), recombinant apo(a); K, kringle; HUVEC, human umbilical vein endothelial cells; r-apo(a), recombinant apo(a); LBS, lysine-binding site; TNFα, tumor necrosis factor-α; ϵ-ACA, ϵ-aminocaproic acid; MLC, myosin light chain; MLCK, MLC kinase; MLCP, MLC phosphatase; RhoK, Rho kinase; LDL, low density lipoprotein; EC, endothelial cell; PBS, phosphate-buffered saline; TRITC, tetramethylrhodamine isothiocyanate.

endothelial barrier function under physiological conditions as well as for the development of barrier failure has been well established (13–15). Various physiological agents such as tumor necrosis factor-α (TNFα), thrombin, oxidized LDL, and Lp(a) have been demonstrated to elicit some manifestations of endothelial barrier dysfunction (16–19). These agents alter the endothelial permeability by stimulating cell contraction through reorganization of the cytoskeleton to increase the size of intercellular gaps and facilitate the entry of inflammatory cells and atherogenic lipoproteins.

A key event in the regulation of endothelial barrier function is actomyosin-driven contraction. EC contraction is initiated by Thr-18/Ser-19 phosphorylation of the 20-kDa regulatory myosin light chain (MLC), which is tightly associated with F-actin filament reorganization (13, 20). Inflammatory agonists such as thrombin and histamine produce rapid increases in MLC phosphorylation, stress fiber formation, and increased endothelial permeability via Rho/Rho kinase-dependent mechanisms (21). Rho-kinase (RhoK) has been proposed to mediate the inhibition of MLC phosphatase (MLCP) via direct phosphorylation of its regulatory subunit (MYPT1) at Thr-696, leading to a net enhancement of MLC phosphorylation in response to various agonists (22, 23). The permeability-augmenting activity of Rho in response to thrombin appears to be mainly mediated by RhoK through its ability to phosphorylate MYPT1, the regulatory subunit of MLCP, thus inactivating this phosphatase (24).

We previously have demonstrated that native Lp(a), through its apo(a) component, elicits rearrangement of the actin cytoskeleton in human umbilical vein endothelial cells (HUVECs) and human coronary artery endothelial cells, characterized by increased central stress fiber formation, dispersion of vascular endothelial (VE)-cadherin, and increased cell permeability (19), whereas treatment with LDL or plasminogen had no effect. These effects were mediated by increased MLC phosphorylation via a Rho/RhoK-dependent signaling pathway; however, the exact mechanisms involved in apo(a)-induced increases in endothelial cell contraction and permeability is not known. In the present study, we first tested the hypothesis that apo(a)-induced stress fiber formation and increased permeability is regulated by Rho/RhoK-driven phosphorylation of MLCP at Thr-696. Next, we utilized a battery of recombinant apo(a) (r-apo(a)) variants in which individual domains were mutated or systematically deleted to define the sequences in apo(a) that mediate endothelial barrier dysfunction. We demonstrate a key functional role for the strong LBS in KIV_{10} of apo(a) in mediating a Rho/RhoK/MYPT1 signaling transduction pathway to enhance MLC phosphorylation via inactivation of MLCP, which thereby increases EC contraction and permeability. Taken together, these results suggest a novel mechanism by which the apo(a) component of Lp(a) can promote endothelial barrier dysfunction during atherogenesis.

EXPERIMENTAL PROCEDURES

Expression and Purification of Recombinant Apo(a)—All of the recombinant apo(a) variants used, with the exception of apo(a) KIV_{1-4}, were cloned and stably expressed in human embryonic kidney (HEK) 293 cells as previously described (25, 26). An expression plasmid encoding the KIV_{1-4} r-apo(a) variant was generated using the parental 17K r-apo(a) expression plasmid pRK5ha17 (26). Apo(a) KIV_{1-4} is purified as previously described with some modifications (27). First, conditioned media containing the recombinant protein was passed over a 5-ml ConA-Sepharose (Amersham Biosciences) micro-column instead of a 20-ml lectin-Sepharose column. The column was washed with HBS containing 0.5 M NaCl, and bound proteins were eluted by the addition of two elution buffers (HBS containing 0.25 M and 0.5 M methyl-α-D-glucopyranoside (Sigma-Aldrich)). Second, the heparin-agarose step was deleted, and the purified KIV_{1-4} was concentrated using centrifugal concentrators (Millipore, 30-kDa NMWL membrane). A schematic diagram of the r-apo(a) variants employed is presented in Fig. 1, along with a silver-stained SDS-PAGE gel demonstrating that all of the variants are of the expected molecular weight.

Double Immunofluorescence—For double immunofluorescence studies, cells were seeded on gelatin-precoated (1 h, 0.1% gelatin (Fisher Scientific) at 37 °C) glass coverslips at a density of 25,000 cells/well in 24-well tissue culture dishes and grown to near confluence. Before treatment with apo(a) variants, cells were washed three times with sterile PBS and serum-starved for 15 min at 37 °C in EBM-2 (Clonetics). This solution was then replaced with fresh EBM-2 containing 200 nM apo(a) variants, and the cells were incubated at 37 °C for 20 min. At this time, the cells were prepared for double immunofluorescence as follows. Cells were fixed with 3.7% paraformaldehyde solution in PBS for 5 min, washed once with PBS, and permeabilized with 1.4% formaldehyde containing 0.1% Nonidet P-40 in PBS for 1.5 min, and then washed with PBS for three times. For F-actin staining, cells were incubated with tetramethylrhodamine isothiocyanate (TRITC)-phalloidin (Sigma-Aldrich) diluted 1:100 in saponin buffer (0.1% saponin, 20 mM KPO_4, 10 mM PIPES, 5 mM EGTA, 2 mM $MgCl_2$, pH 6.8). For simultaneous staining of F-actin and VE-cadherin, cells were incubated with anti-VE-cadherin monoclonal antibody (Research Diagnostics) diluted 1:350 in saponin buffer for 1 h at room temperature. Following three washes with PBS, cells were incubated for 1 h with 1:500-diluted goat anti-mouse Alexa488-conjugated antibody (Molecular Probes) and TRITC-phalloidin in saponin buffer in the dark. Following three washes with PBS, coverslips were mounted to slides using an anti-fade mounting solution (Dako) and examined using a Zeiss Axiovert S100 inverted fluorescence microscope equipped with a 40× oil immersion lens. Images were captured using a high sensitivity Cooke SensiCam and SlideBook software (Intelligent Imaging Innovations Inc.).

Transendothelial Permeability Assay—Cells were seeded (300 μl) at a final concentration of 25,000 cells/ml onto Transwell inserts (0.4-μm pore size, BD Biosciences) precoated with 7 μg/ml fibronectin (1 h, 37 °C) and placed into 24-well Transwell companion plates (BD Biosciences) containing 700 μl of the complete medium (EGM-2, Clonetics). Cells were grown for 3–4 days with one change of medium before the experiment. The level of confluence of the cells was checked before the treatment by fixation and Coomassie Blue staining of the

cells in one of the Transwell inserts. When the cells were near confluence, medium in the top well was replaced with EGM-2 containing 1 mg/ml fluorescein isothiocyanate-dextran (molecular weight, 40,000) in a final volume of 100 μl; some wells also received 400 nM apo(a) variants or 1 μg/ml TNFα (as a positive control). The medium in the bottom well was replaced with 600 μl of fresh EGM-2. At specific time points, 50 μl of medium from the bottom well was removed and replaced with 50 μl of fresh EGM-2. The removed sample was diluted with 950 μl of PBS, and fluorescence intensity was measured with a fluorometer (PerkinElmer Life Sciences LS-50B) using an excitation wavelength of 492 nm and emission wavelength of 520 nm.

MLC Phosphorylation—MLC phosphorylation was analyzed by SDS-PAGE followed by Western blotting. HUVECs were grown to near confluence in 6-well tissue culture plates and treated with 400 nM apo(a) variants for different times. The incubations were terminated by addition of 1.5 ml of ice-cold 10% trichloroacetic acid. Cells were scraped into microcentrifuge tubes and centrifuged for 20 min at 14,000 $\times$ *g*. Supernatants were discarded, and pellets were washed three times (20 min at 14,000 $\times$ *g*) with water to remove residual trichloroacetic acid. Resulting pellets were resuspended in 1% SDS and then sonicated overnight at 4 °C. Samples were subjected to SDS-PAGE on a 15% polyacrylamide gel, and resolved proteins were transferred to Immobilon P membranes (Millipore) in transfer buffer (25 mM Tris, 192 mM glycine, 10% methanol). Membranes were blocked with 6% skim milk powder in 1× NET (150 mM NaCl, 5 mM EDTA, 50 mM Tris, 0.05% Triton X-100, pH 7.4) overnight at room temperature, washed once in 1× NET, and probed for either phosphorylated MLC with 1:750-diluted anti-phospho-MLC antibody (Thr-18/Ser-19, Santa Cruz Biotechnology) or for total MLC with 1:200-diluted total MLC antibody (FL-172, Santa Cruz Biotechnology) for 1 h at room temperature. Membranes were then washed three times with 1× NET and incubated with 1:2500 dilutions of the appropriate horseradish peroxidase-conjugated secondary antibodies (Santa Cruz Biotechnology) in 1× NET for 1 h at room temperature. Membranes were then washed three times with 1× NET. Finally, membranes were developed with chemiluminescence (ECL) Western blotting detection reagents (Amersham Biosciences) and exposed to x-ray film. Blots were scanned using a flatbed laser scanner, and the density of the immunoreactive bands was determined using Corel PHOTO-PAINT Version 10. The amount of phosphorylated MLC was normalized to the total MLC signal in the respective samples.

MLC Phosphatase Phosphorylation—HUVECs were grown to confluence in a 6-well tissue culture plates. HUVECs were lysed in a lysis buffer (50 mM Tris-HCl, pH 7.4, 1% Nonidet P-40, 0.25% sodium deoxycholate, 150 mM NaCl, 1 mM EDTA, 1 mM phenylmethylsulfonyl fluoride, 1 μg/ml aprotinin, 1 μg/ml leupeptin, 1 μg/ml pepstatin, 1 mM Na_3VO_4, 1 mM NaF). SDS-PAGE using a 7% polyacrylamide gel was followed by Western blot as described in the manufacturers' protocol (Upstate Biotechnology). Membranes were probed either by using anti-MYPT1 rabbit polyclonal IgG or anti-phospho-MYPT1 (Thr-696) rabbit polyclonal IgG (Upstate). Washed membranes were incubated with appropriate anti-rabbit horseradish peroxidase-conjugated secondary antibody (1:2500 dilutions, Santa Cruz Biotechnology). Then, membranes were developed using enhanced chemiluminescence (Millipore or Amersham Biosciences) Western blotting detection reagents for phospho-MYPT1 or total-MYPT1, respectively. Densitometry of the bands was performed using Corel PHOTO-PAINT version 10. The amount of phosphorylated MYPT1 was normalized to the total MYPT1 signal in the respective samples.

Rho Activation Assay—Rho activation was determined as described in the manufacturers' protocol (Upstate Biotechnology). Briefly, HUVECs were grown to ~90% confluence in 100-mm tissue culture plates and treated with 200 nM 17K or 17KΔAsp for designated times. Cells were washed with ice-cold Tris-buffered saline twice. At this time, ice-cold Mg^{2+} lysis buffer (25 mM HEPES, pH 7.5, 150 mM NaCl, 1% Igepal CA-630, 50 mM $MgCl_2$, 1 mM EDTA, 2% glycerol, 25 mM NaF, 1 mM Na_3VO_4) was added, and the cell lysates were scraped into microfuge tubes on ice. After 15 min at 4 °C with agitation, the lysates were incubated with Rhotekin RBD-agarose for 45 min. After brief centrifugation, supernatant were collected, and 2× SDS-PAGE sample buffer was added. The pelleted agarose beads were washed three times with Mg^{2+} lysis buffer and were resuspended in 2× Laemmli reducing sample buffer. SDS-PAGE using 12% polyacrylamide gel was followed by Western blot analysis as described in the manufacturer's protocol (Upstate Biotechnology). Membranes were probed either by using mouse IgG_1 anti-Rho (-A, -B, and -C) for the pelleted samples or mouse polyclonal anti-β-actin (Sigma) for the supernatants. Washed membranes were incubated with appropriate anti-mouse horseradish peroxidase-conjugated secondary antibody (1:2500 dilutions, Santa Cruz Biotechnology). Membranes were developed using ECL reagents (Amersham Biosciences).

RESULTS

Recombinant Apo(a) Stimulates F-actin Stress Fiber Formation in HUVECs—Previous studies have demonstrated that apo(a) and Lp(a) increases F-actin stress fiber formation. To illustrate which domain or domains in apo(a) stimulate these effects, we have expressed and purified a battery of r-apo(a) variants representing systematic deletions and mutations of key domains in the molecule. 17K r-apo(a) (17K) contains all of the domains found in apo(a) and in fact represents a physiologically relevant isoform with eight copies of KIV_2 domains (22). 17KΔAsp contains an amino acid substitution that abolishes the strong LBS in KIV_{10}, whereas 17KΔV represents a deletion of entire KV domain (Fig. 1).

Following a brief 15-min serum starvation, confluent HUVECs displayed few actin stress fibers and possessed VE-cadherin molecules organized as slender lines along the margins of the cells (Fig. 2*A*). Actin stress fibers were formed mostly along the cell borders and were generally absent in the central regions of the cells. The stimulatory effect of various 17K concentrations (100 nM to 400 nM) was observed after 5 min of incubation and was sustained until 30 min of incubation (data not shown). Therefore, a 20-min incubation of 200 nM r-apo(a) was used for subsequent immunofluorescent experiments. Treatment with 200 nM 17K resulted in an increased number of

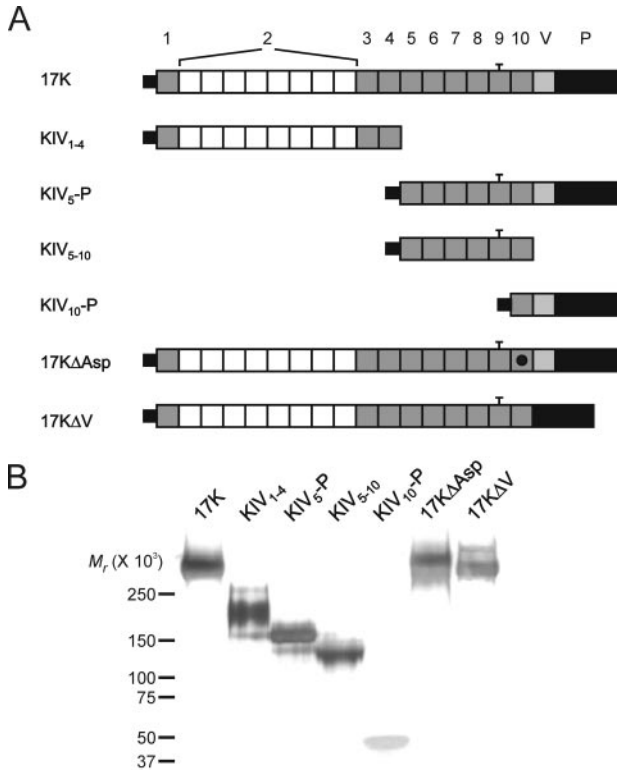

FIGURE 1. **Recombinant apo(a) variants used in this study.** *A*, schematic diagram shows the topology of r-apo(a) variants. *17K* represents a physiologically relevant apo(a) isoform and contains all of the kringle domains present in all apo(a) isoforms. The numbering of KIV types is provided at the *top*. The *black dot* in the KIV_{10} domain in 17KΔAsp represents a single amino acid substitution, which abolishes the strong LBS in this kringle. The *bar* over KIV_9 represents an unpaired cysteine residue in this kringle. *B*, 1 μg of each of the purified r-apo(a) variants was subjected to SDS-PAGE on a 2.5–15% polyacrylamide gradient gel. The gel was silver-stained. The migration of molecular weight standards is indicated to the *left* of the gel.

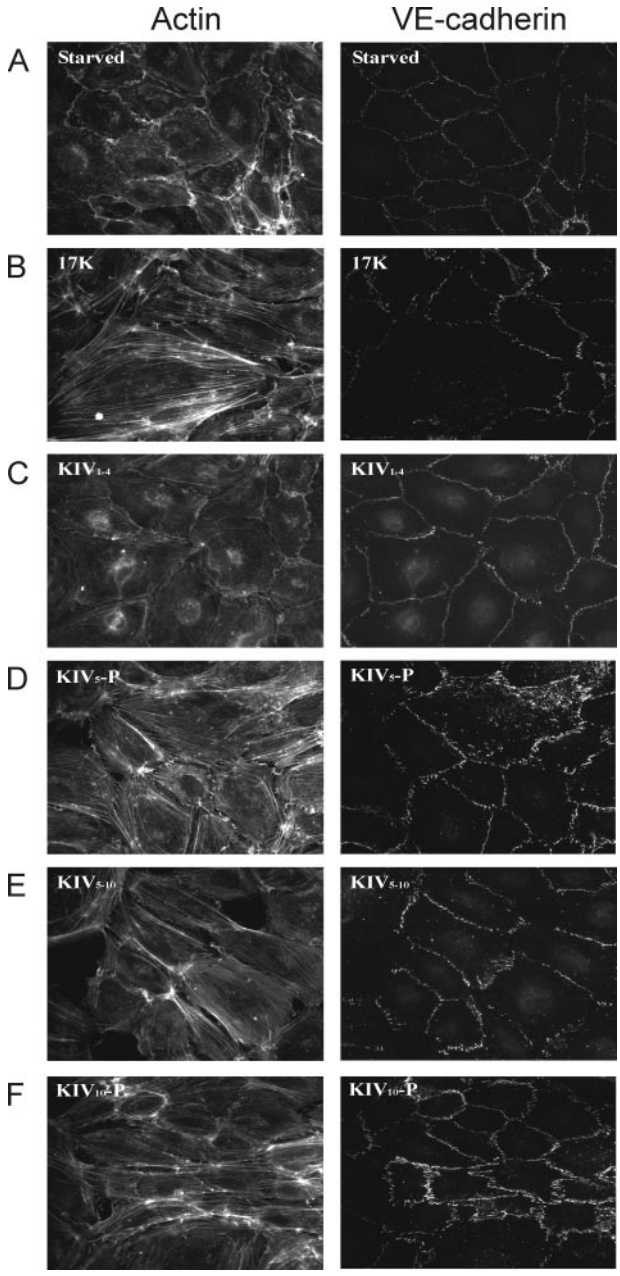

FIGURE 2. **KIV_{10} is required for apo(a)-induced cytoskeletal reorganization in HUVECs.** HUVECs were serum-starved for 15 min (*A*) and then treated with 200 nM of r-apo(a) variants (17K, IV_{1-4}, KIV_5-P, KIV_{5-10}, and KIV_{10}-P) for 20 min (*B–F*, respectively). Cells were fixed, permeabilized, and stained for F-actin (*left*) and VE-cadherin (*right*) using TRITC-phalloidin and a monoclonal anti-VE-cadherin antibody followed by an Alexa-488-linked secondary antibody, respectively.

F-actin stress fibers traversing the cells and, concomitantly, a dispersed VE-cadherin appearance with evident intercellular gap formation (Fig. 2*B*). For an Lp(a) isoform containing a 17-kringle form of apo(a), a molar concentration of 100 nM corresponds to a mass concentration of ~30 mg/dl, which is often cited as the apparent risk threshold for Lp(a) concentrations. Therefore, the effects of apo(a) observed here occur at physiologically relevant concentrations.

We next examined the ability of each of our r-apo(a) deletion constructs to enhance stress fiber formation and VE-cadherin dispersion (Fig. 2, *C–F*). We first tested variants encompassing the N-terminal (KIV_{1-4}) and C-terminal (KIV_5-P) domains of 17K r-apo(a). Only KIV_5-P had increased both stress fiber formation and VE-cadherin dispersion, whereas KIV_{1-4} had no effect, suggesting a possible role of C-terminal end of this molecule (Fig. 2, *C* and *D*). In addition to 17K and KIV_5-P, two other variants (KIV_{5-10} and KIV_{10}-P) containing C-terminal sequences elicited stress fiber formation leading to endothelial intercellular gap formation (Fig. 2, *E* and *F*). Interestingly, KIV_{10} was the only kringle that was commonly shared in all four positive effectors (17K, $KIV_{5\text{-}P}$, KIV_{5-10}, and $KIV_{10\text{-}P}$). Accordingly, the 17KΔAsp variant in which the strong LBS in KIV_{10} was mutated had no effect on stress fiber formation and VE-cadherin dispersion (Fig. 3*C*). 17KΔV, which lacks KV and its weak LBS, had similar effects on stress fiber formation and VE-cadherin dispersion to 17K (Fig. 3*D*).

F-Actin Stress Fiber Stimulation and VE-cadherin Dispersion by Apo(a) Leads to Increase in Vascular Endothelial Permeability and Is Mediated by a Rho Kinase and Lysine-dependent Pathway—We hypothesized that the increase in stress fiber formation and loss of cell-cell contact via disruption of VE-cadherin organization following an r-apo(a) exposure leads to enhanced trans-endothelial permeability. Consistent with this hypothesis, treatment of HUVEC monolayers with 200 nM 17K resulted in an increase in trans-endothelial diffusion of fluores-

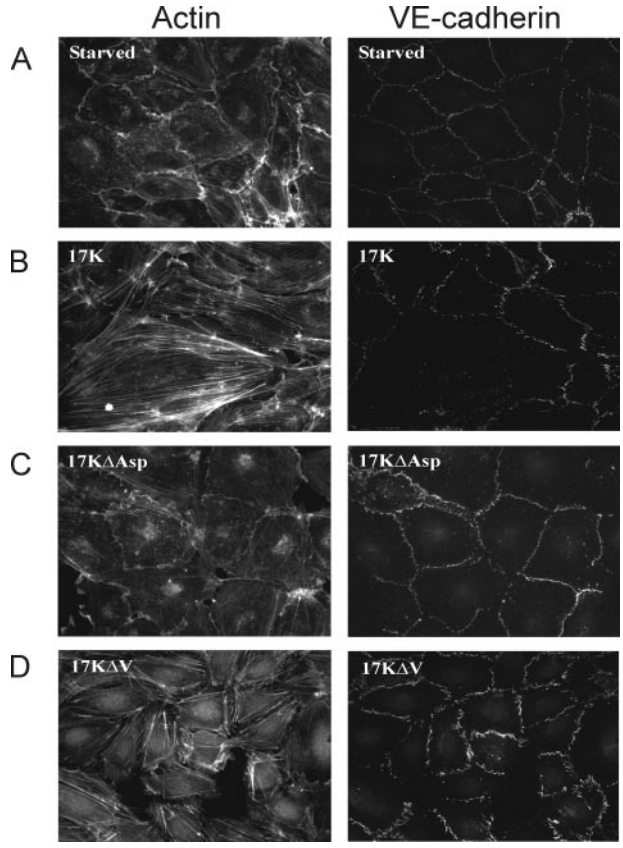

FIGURE 3. **The strong lysine-binding site in KIV_{10} is required for stimulation of F-actin stress fibers and VE-cadherin dispersion.** HUVECs were serum-starved for 15 min (*A*) and then treated with 200 nM of r-apo(a) variants (17K, 17KΔAsp, and 17KΔV) for 20 min (*Panels B–D*, respectively). Cells were then fixed, permeabilized, and stained for F-actin (*left*) and VE-cadherin (*right*) using TRITC-phalloidin and a monoclonal anti-VE-cadherin antibody followed by an Alexa-488-linked secondary antibody, respectively. The data in *A* and *B* are identical to that in the corresponding *panels* in Fig. 2.

cein isothiocyanate-dextran that peaked after 1 h and was maintained at this level for 8 h (Fig. 4*A*); TNFα and plasminogen were used as positive and negative controls, respectively (16, 19). In accordance with the results seen for stress fiber formation and VE-cadherin dispersion, all the deletion constructs that contain KIV_{10} (KIV_5-P, KIV_{5-10}, and KIV_{10}-P) resulted in a significant increase in transendothelial permeability after 1 h of treatment where KIV_{1-4} had no effect (Fig. 4, *B* and *C*). Consistent with its lack of effects on stress fiber formation and VE-cadherin dispersion, 17KΔAsp did not increase EC permeability. Interestingly, 17KΔV resulted in a delayed increase in permeability, only reaching significance after 4 h (Fig. 4*D*). In keeping with the apparent dependence on the strong LBS in KIV_{10} for the effects of apo(a), addition of 80 mM ϵ-ACA, a lysine analogue, totally abolished 17K-induced EC permeability (Fig. 4*E*), as did the addition of a pharmacological RhoK inhibitor (Y27632, 5 μM). These findings indicate that apo(a) increases EC permeability via a pathway dependent on cell surface lysines and intracellular signaling through RhoK.

Enhancement of MLC Phosphorylation by r-Apo(a) Variants Is Time-dependent and Is Mediated by a Rho Kinase and Lysine-dependent Pathway—Phosphorylation of MLC at Thr-18/Ser-19 is required for myosin II activation and stress fiber formation, leading to an increase in EC contraction and permeability (13). We have previously shown that treatment with apo(a) resulted in rapid increase in MLC phosphorylation in a Rho/RhoK-dependent manner (19). In determining which the domain(s) in apo(a) mediate an increase in MLC phosphorylation, HUVECs were exposed to r-apo(a) and the extent of MLC phosphorylation was analyzed by Western blot analysis. As can be seen in Fig. 5*A*, treatment with 200 nM 17K showed maximal MLC phosphorylation (~3-fold higher than untreated control cells) between 2 and 5 min of stimulation; 17K concentrations below 100 nM did not, however, induce MLC phosphorylation (data not shown). Thrombin (0.5 unit/ml) and plasminogen (400 nM) were used as positive and negative controls, respectively (Fig. 5*A*). After 5 min of 17K treatment, the extent of MLC phosphorylation decreased at a level that remained higher than the levels observed in the control. In agreement with the F-actin/VE-cadherin and permeability data, both KIV_{5-10} and KIV_{10}-P elicited a significant increase in MLC phosphorylation, whereas KIV_{1-4} and 17KΔAsp did not (Fig. 5, *B* and *C*). KIV_{5-10} treatment resulted in maximal MLC phosphorylation at 2 min, which reduced rapidly to a level similar to that of untreated cells, whereas KIV_{10}-P did not result in increased MLC phosphorylation until 10 min of treatment, after which time it remained at a level comparable to that elicited by 17K (Fig. 5*B*). KIV_{1-4} and 17KΔAsp did not induce MLC phosphorylation, indicating a critical role for the strong LBS in KIV_{10} in MLC phosphorylation (Fig. 5, *B* and *C*). Consistent with a delayed increase in EC permeability (Fig. 4*D*), 17KΔV elicited a transient increase in MLC phosphorylation that was slightly lower than that elicited by 17K (Fig. 5*C*). An apo(a) variant that lacks the weak LBS in KV domain elicited the same effect on MLC phosphorylation as did 17KΔV (data not shown); along with the transient increase elicited by KIV_{5-10}, this suggests a specific role for the weak LBS in KV in sustaining the MLC phosphorylation state induced by apo(a). Treatment with ϵ-ACA completely inhibited 17K-induced increase in MLC phosphorylation in a dose-dependent manner (Fig. 5*D*). On the other hand, thrombin-induced MLC phosphorylation was not affected at all by 80 mM ϵ-ACA treatment (data not shown).

Inhibition of RhoK by Y27632 totally abolished the 17K-mediated enhancement of MLC phosphorylation (Fig. 5*D*); inhibition of RhoK also completely blocked KIV_{5-10}- and KIV_{10}-P-mediated increases in MLC phosphorylation (data not shown). Kawano and coworkers (28) have suggested that RhoK activation increases MLC phosphorylation by two potential mechanisms: direct phosphorylation of MLC Thr-18/Ser-19 and indirectly via phosphorylation of the regulatory subunit of myosin phosphatase (MYPT1) at Thr-696. ML-7 (an MLCK inhibitor) totally blocked the phosphorylation of MLC induced by 17K, indicating that only MLCK and not RhoK is responsible for the enhanced MLC phosphorylation elicited by apo(a) (Fig. 5*D*).

Elevated MLCP Phosphorylation at Thr-696 By r-Apo(a) Variants Is Mediated by a RhoK and Lysine-dependent Pathway—RhoK inactivates myosin phosphatase via phosphorylation of its 130-kDa regulatory subunit (MYPT1) at Thr-696 (28); as such, RhoK serves to promote, albeit indirectly, MLCK-mediated MLC phosphorylation. Therefore, we assessed whether apo(a) could influence the extent of MYPT1 phospho-

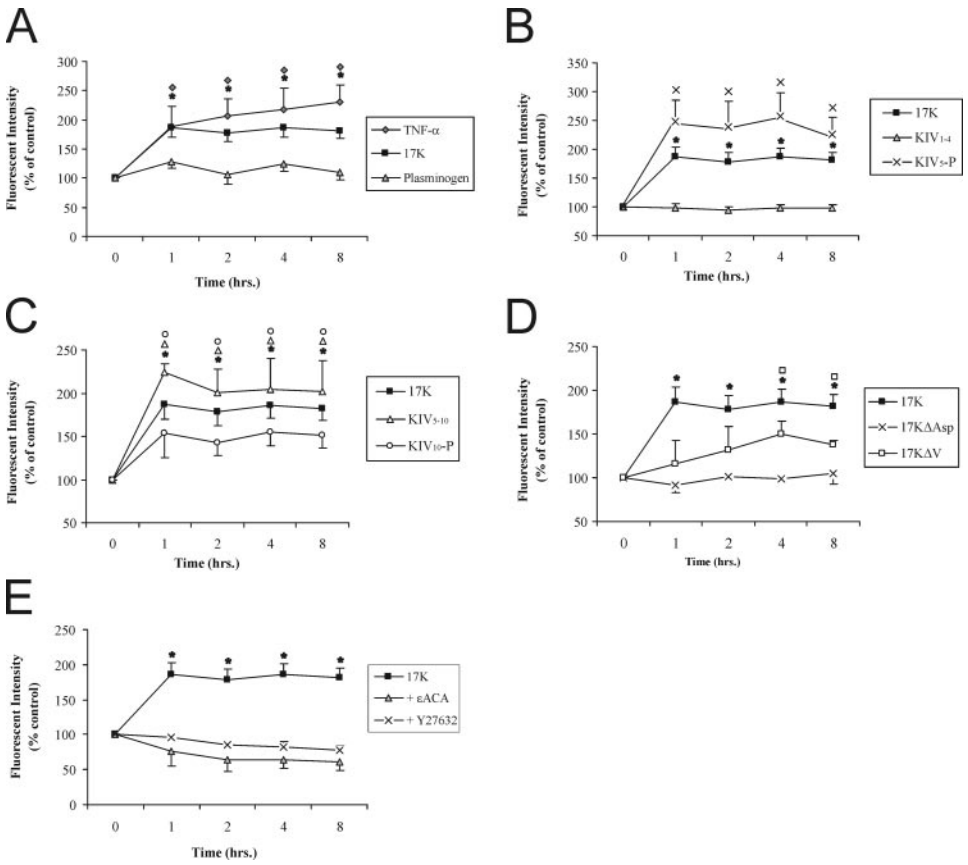

FIGURE 4. **Kringle IV type 10 containing r-apo(a) variants increase endothelial cell permeability in a lysine- and a RhoK-dependent manner.** HUVECs were treated with serum-depleted medium (control) or serum-depleted medium containing 200 nM r-apo(a) variants for the indicated time periods. Transendothelial permeability was determined fluorometrically as described under "Experimental Procedures." Results represent the mean ± S.E. of four independent measurements. All the data were normalized to initial permeability and then to the control. The *asterisks* represent the increases in EC permeability in the presence of 17K r-apo(a) that are significantly different ($p < 0.05$) from those in the absence of 17K. Other *symbols* over the *plots* represent significant differences ($p < 0.05$) for r-apo(a) variants represented by the corresponding plot symbols in each *panel* (as shown in the legends). *A*, comparison of 17K treatment with TNFα (positive control) and plasminogen (negative control). *B*, comparison of 17K treatment with KIV_5-P and KIV_{1-4}. *C*, comparison of 17K, KIV_{5-10}, and KIV_{10}-P treatments. *D*, comparison of 17K, 17KΔV, and 17KΔAsp. *E*, 17K treatment was carried out in the presence of 5 μM Y27632 (cell were pretreated with this compound for 1 h) or 80 mM ε-ACA. In *B–E*, the 17K data are identical to that in *A*.

rylation at Thr-696 in HUVECs. Treatment with 200 nM 17K resulted in a significant increase in MYPT1 phosphorylation at Thr-696 in a time-dependent manner with maximum at 2 min (Fig. 6*A*); the extent of MYPT1 phosphorylation then decreased to basal levels or below after ~8 min (Fig. 6*A*). Consistent with their effects on HUVEC permeability and MLC phosphorylation, KIV_{5-10}, $KIV_{10\text{-}P}$, and 17KΔV also stimulated MLCP phosphorylation at Thr-696, in a manner similar to 17K (Fig. 6, *B* and *C*). Similarly, KIV_{1-4} and 17KΔAsp failed to induce any effect on MYPT1 phosphorylation (Fig. 6*C*). Inhibition of RhoK completely abolished 17K-induced MYPT1 phosphorylation as expected (Fig. 6*D*), as well as that mediated by KIV_{5-10} and $KIV_{10\text{-}P}$ (data not shown). The addition of ε-ACA completely abolished 17K-induced MYPT1 phosphorylation (Fig. 6*D*), in agreement with the importance of the strong LBS in mediating this effect as revealed by the results with KIV_{1-4} and 17KΔAsp.

17K, but Not 17KΔAsp, Activates Rho—Having shown that apo(a), in a manner dependent on the strong LBS in KIV_{10}, induces MLCP inactivation through RhoK phosphorylation of MYPT1, we directly assessed if apo(a) is able to activate Rho. HUVECs were treated with either 17K or 17KΔAsp, and cell lysates were prepared at different times for the measurement of the relative amount of active (GTP-bound) Rho. In agreement with the preceding data, 17K, but not the 17KΔAsp variant, stimulated the formation of GTP-bound Rho, with the peak amounts of GTP-Rho observed between 5 and 10 min of apo(a) treatment (Fig. 7). These data confirm that apo(a), through its strong LBS in KIV_{10}, induces cytoskeleton rearrangement and a subsequent increase in EC permeability through a Rho/RhoK/MYPT1-dependent pathway.

DISCUSSION

Elevated plasma concentrations of Lp(a) have been considered as a risk factor for the development of a variety of atherogenic disorders, including coronary heart disease (1, 2). Considerable evidence has emerged to suggest that Lp(a) is a proatherogenic effector (1, 2); however, the exact mechanisms by which it exerts its pathogenic effects remain unclear. Because plasma Lp(a) levels are relatively resistant to most pharmacological lipid lowering therapy or dietary interventions (29, 30), it is critical to elucidate the mechanisms of Lp(a) action as they may be potential targets for therapeutic interventions.

One means to evaluate which of the functions of Lp(a) are most significant *in vivo* is to determine what functional domains of apo(a) mediate the respective functions. Indeed, it has already been demonstrated that mice expressing an apo(a) variant lacking the strong LBS in KIV_{10} are less susceptible to atherosclerosis than mice expressing wild-type apo(a) (31). We show in the current study that this LBS is absolutely required to mediate the effects of apo(a) on actin cytoskeletal rearrangements in cultured HUVECs that culminate in enhanced endothelial permeability, a critical early event in the atherosclerotic process.

Lp(a) has been shown to affect a variety of endothelial cell functions. Lp(a) has been shown to trigger mononuclear cell adherence by inducing the expression of a number of adhesion molecules on endothelial cells such as vascular cell adhesion molecule-1, intracellular adhesion molecule-1, P-selectin, and E-selectin (32–34). Apo(a) also induces the expression of the CC chemokine I-309, a monocyte chemoattractant, in endothelial cells (35). Elevated Lp(a) concentrations in plasma also

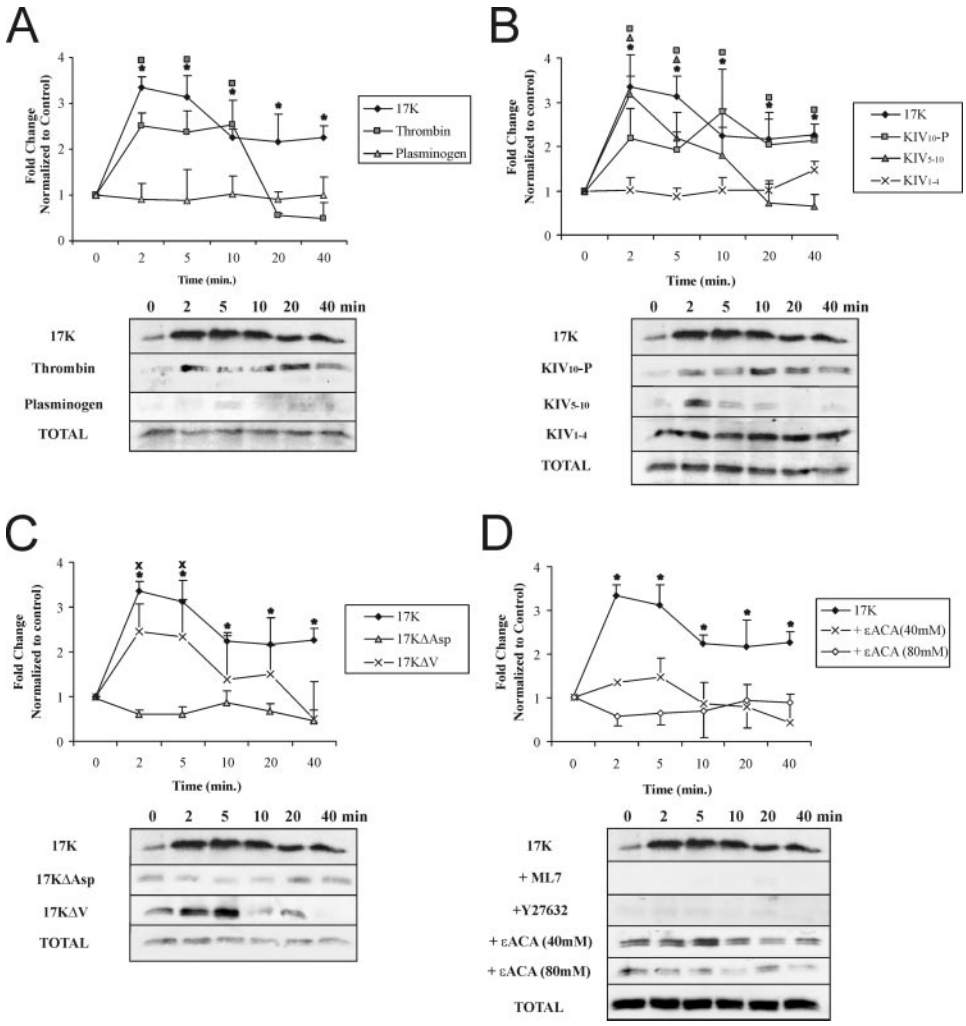

FIGURE 5. **Kringle IV type 10 containing r-apo(a) variants increase MLC phosphorylation in a lysine-, RhoK-, and MLCK-dependent manner.** HUVECs were serum-starved for 15 min and then treated with 200 nM r-apo(a) variants for the indicated time periods. Total cellular proteins were harvested and subjected to Western blot analysis using anti-phospho-MLC (*p-MLC*) and anti-total MLC antibody (*Total-MLC*). *Graphs* in each *panel* show mean band density (normalized to the control) ± S.E. of at least three independent experiments, and representative Western blots are shown below. The *asterisks* represent increases in MLC phosphorylation in the presence of 17K r-apo(a) that are significantly different ($p < 0.05$) from those in the absence of 17K. *Other symbols* over the *plots* represent significant differences ($p < 0.05$) from the normalized control of individual r-apo(a) variant represented by the corresponding plot symbols in each *panel* (as shown in the legends). *A*, comparison of 17K treatment with TNFα (positive control) and plasminogen (negative control). *B*, comparison of 17K treatment with deletion mutants (KIV1–4, KIV10-P, and KIV5–10). *C*, comparison of 17K treatment with point mutants (17KΔV and 17KΔAsp). *D*, 17K treatment was carried out in the presence of ML-7 or Y27632 (5 μM each; cells were pretreated with each compound for 1 h) or ϵ-ACA (80 mM).

by Lp(a). The present study considerably extends these findings.

Endothelial cells are equipped with contractile apparatus, which is involved in cell shape change, motility, and endothelial permeability regulation. The process of EC contraction and intercellular gap formation appears to be controlled by actin-myosin interaction via Ca^{2+}/CaM-depenent MLC phosphorylation (20). Inhibition of MLCP via a Rho-dependent mechanism contributes to increased MLC phosphorylation, endothelial contraction, and permeability (24). Phosphorylation of the MYPT1 regulatory site by RhoK induces inhibition of MLCP activity (22, 23). Using site-specific antibodies to phospho-MYPT1 at Thr-696 and total MYPT1, we demonstrated that 17K stimulation enhanced MYPT1 phosphorylation (Fig. 6). Direct involvement of the Rho-RhoK-MYPT1 pathway in 17K-induced MLC phosphorylation and cytoskeletal remodeling was clearly demonstrated in our study, because pharmacological inhibition of RhoK by Y27632 abolished the 17K-induced increases in MYPT1 phosphorylation at Thr-696 (Fig. 6) MLC phosphorylation at Ser-18/Thr-19 (Fig. 5), and EC permeability (Fig. 4). Moreover, we have demonstrated, for the first time, that apo(a) elicits an increase in Rho activation (Fig. 7). Consistent with these data, we previously have demonstrated that Rho inactivation by C3-exotoxin-induced ADP-ribosylation or overexpression of dominant-negative Rho attenuated 17K-induced stress fiber formation and VE-cadherin dispersion (19). Furthermore, the addition of pharmacological MLCK inhibitor (ML-7) completely abolished 17K-induced MLC phosphorylation, which suggests the direct phosphorylation of MLC by RhoK is not possible. Interestingly, 17K had failed to increase intracellular Ca^{2+} levels (19), indicating that the activity of MLCK would not be altered by apo(a). Taken together, 17K-induced endothelial barrier dysfunction is mediated by indirect activation of myosin II via Rho-RhoK-MYPT1 pathway that inactivates MLCP. This results in an increase in MLC phosphorylation and stress fiber formation and thus an increase in EC permeability.

In the present study, we have established a novel finding that the strong LBS in apo(a) kringle IV type 10 is absolutely required for apo(a)-mediated changes in cytoskeletal rear-

appear to evoke endothelial dysfunction *in vivo*: clinical studies have demonstrated impaired endothelium-dependent vasodilation in hypercholesterolemic children with high Lp(a) (36). Similarly, elevation in Lp(a) levels has been associated with impairment of receptor-mediated endothelial vasodilation in adult subjects (37, 38). Our own studies using cultured human umbilical vein or coronary artery endothelial cells revealed a novel effect of Lp(a) that was mediated by its apo(a) component: impairment of the barrier function of endothelial cells through cell contraction occurring as a consequence of a rearrangement of the actin cytoskeleton (19). We determined that apo(a) resulted in an increase in MLC phosphorylation through a Rho/RhoK-dependent pathway. This was the first report of an intracellular signaling pathway in endothelial cells that was triggered

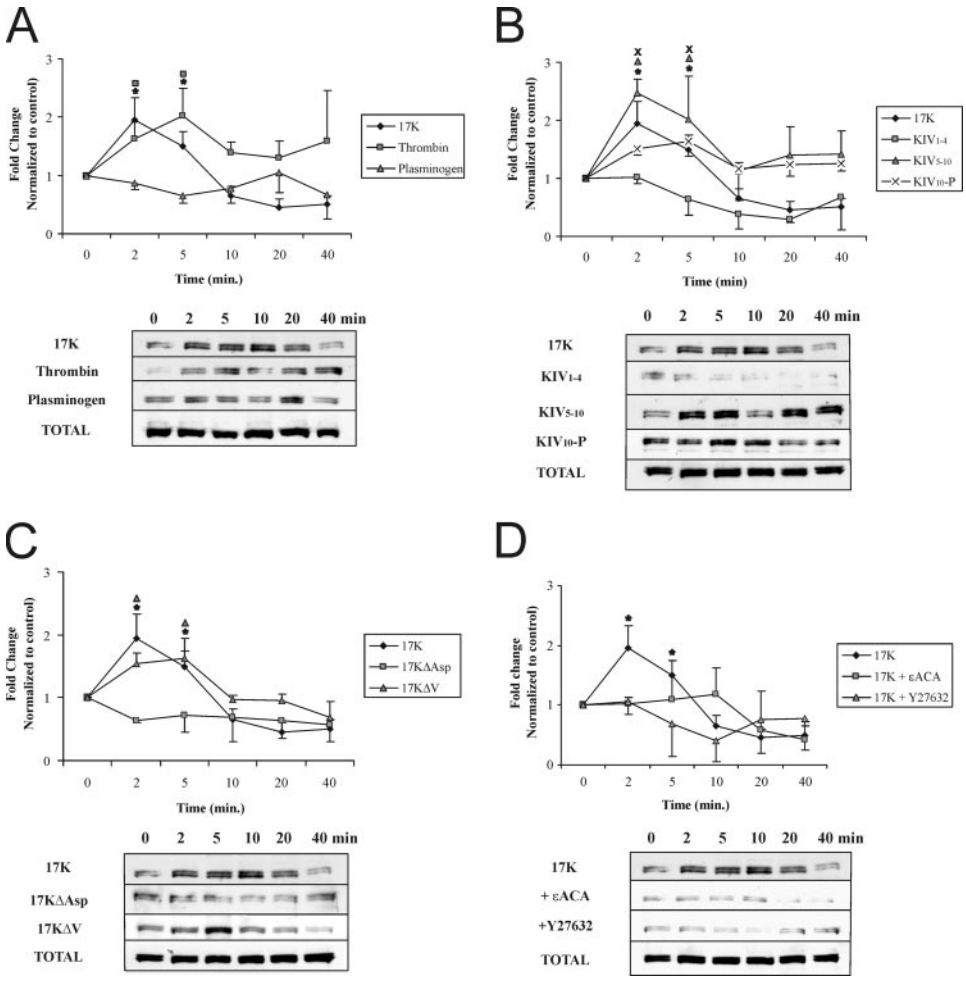

FIGURE 6. **Kringle IV type 10 containing r-apo(a) variants increase MYPT1 phosphorylation in a lysine- and RhoK-dependent manner.** HUVECs were serum-starved for 15 min and then treated with 200 nM r-apo(a) variants for the indicated time periods. Total cellular proteins were harvested and subjected to Western blot analysis using anti-phospho-MYPT1 (p-MYPT1) and anti-total-MYPT1 (Total-MYPT1). *Graphs* in each *panel* show mean band density (normalized to the control) ± S.E. of three independent experiments, and representative Western blots are shown below. The *asterisks* represent increases in MYPT1 phosphorylation in the presence of 17K r-apo(a) that are significantly different ($p < 0.05$) from those in the absence of r-apo(a) variants. *Other symbols* over the *plots* represent significant differences ($p < 0.05$) from the normalized control of each r-apo(a) variant represented by the corresponding plot symbols in each *panel* (as shown in the legends). *A*, comparison of 17K treatment with TNFα (positive control) and plasminogen (negative control). *B*, comparison of 17K treatment with deletion mutants (KIV1–4, KIV10-P, KIV5–10). *C*, comparison of 17K treatment with point mutants (17KΔV and 17KΔAsp). *D*, 17K treatment was carried out in the presence of Y27632 (5 μM; cells were pretreated with this compound for 1 h) or ϵ-ACA (80 mM).

rangements. We showed that all KIV_{10}-containing r-apo(a) variants (17K, KIV_5-P, KIV_{5-10}, and KIV_{10}-P) stimulated F-actin stress fiber formation, VE-cadherin dispersion, MLC phosphorylation, MYPT1 phosphorylation, and EC permeability, whereas variants lacking KIV_{10} or its strong LBS (KIV_{1-4} and 17KΔAsp, respectively) and plasminogen had no effect on any of these parameters. Furthermore, addition of ϵ-ACA completely abolished all of 17K-induced effects, indicating that the role of lysine-binding sites within apo(a) molecule is essential.

In addition to the strong LBS in KIV_{10}, apo(a) contains weaker LBS in KIV_{5-8} and KV. Based on the properties of variants that lack these domains (KIV_{10}-P and 17KΔV, respectively), none of these weak LBS appear to play a crucial role in the effects of apo(a) on endothelial cells, although these variants displayed somewhat reduced potencies with respect to some parameters (Figs. 4–6). We have previously shown that the 17KΔV variant is unable to inhibit tissue plasminogen activator-mediated plasminogen activation in the context of fibrin (39). Moreover, the KV domain may affect the conformation of the apo(a) molecule: baboon Lp(a) does not bind to lysine-Sepharose despite the presence of a functional strong LBS in KIV_{10} and baboon apo(a) lacks KV (40). In the current study, it appears that it is the weak LBS in KV that accounts for the contribution of this kringle to the maximal effects of apo(a), because treatment with a variant containing a point mutation in the KV weak LBS showed very similar effects on MLC phosphorylation and EC permeability as treatment with 17KΔV (data not shown). Nonetheless, it is the strong LBS in KIV_{10} that is absolutely required for the effects of apo(a) on the HUVEC cytoskeleton.

Our working hypothesis is that apo(a) interacts in a lysine-dependent manner with an as yet unidentified receptor in endothelial cells to facilitate downstream signaling events. Given the short time (<5 min) required to observe effects of apo(a) on the cytoskeleton, it is unlikely that changes in gene expression are involved. The most obvious possibility is that apo(a) binds to one of the plasminogen receptors. These receptors exist primarily to modulate pericellular plasminogen activation, and are represented by both protein (α-enolase, the S100A10 component of the annexin A2-S100A10 heterotetramer) and non-protein (gangliosides) cell surface moieties (41, 42). Of the protein receptors, only annexin A2 has been linked to Rho activation or the actin cytoskeleton (43). Certain gangliosides are components of lipid rafts, which can serve to cluster active Rac and Rho (44–46). Both of these GTPases were found to be critical for mediating the effects of apo(a) in our previous work (19). However, we have shown that plasminogen has absolutely no effect on actin cytoskeleton reorganization, signaling to the actin cytoskeleton, or cell permeability (Ref. 19 and Figs. 4–6). Therefore, it is clear that apo(a) either interacts with a plasminogen receptor in a different manner than plasminogen itself to mediate these effects, or apo(a) acts through a novel receptor.

In summary, we have characterized the biochemical pathways leading to EC barrier dysfunction induced by apo(a) in a manner dependent on the strong LBS in KIV_{10}. Our working model is as follows (Fig. 8): apo(a), through its sLBS in KIV_{10},

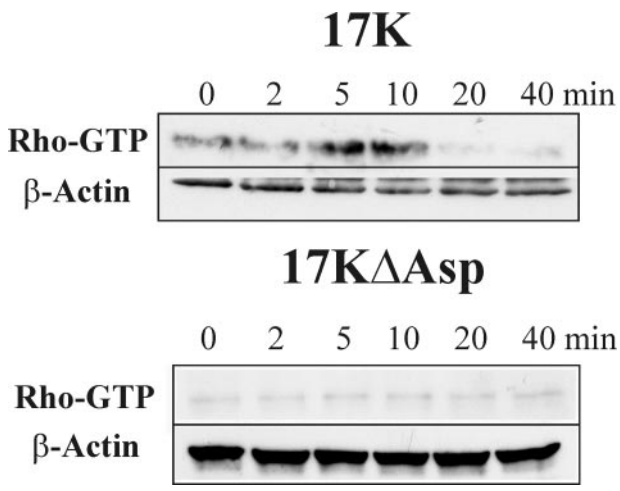

FIGURE 7. **Stimulation of Rho activation by apo(a) requires the strong LBS in KIV$_{10}$.** HUVECs were serum-starved for 15 min and treated with 200 nM 17K or 200 nM 17KΔAsp for the indicated time periods. Total cellular proteins were harvested and subjected to a Rho-GTP pull down assay as described under "Experimental Procedures." Then, Western blot analyses were performed using anti-Rho for GTP-Rho as well as anti-β-actin as a loading control. Representative Western blots of three independent experiments for both 17K and 17KΔAsp are shown.

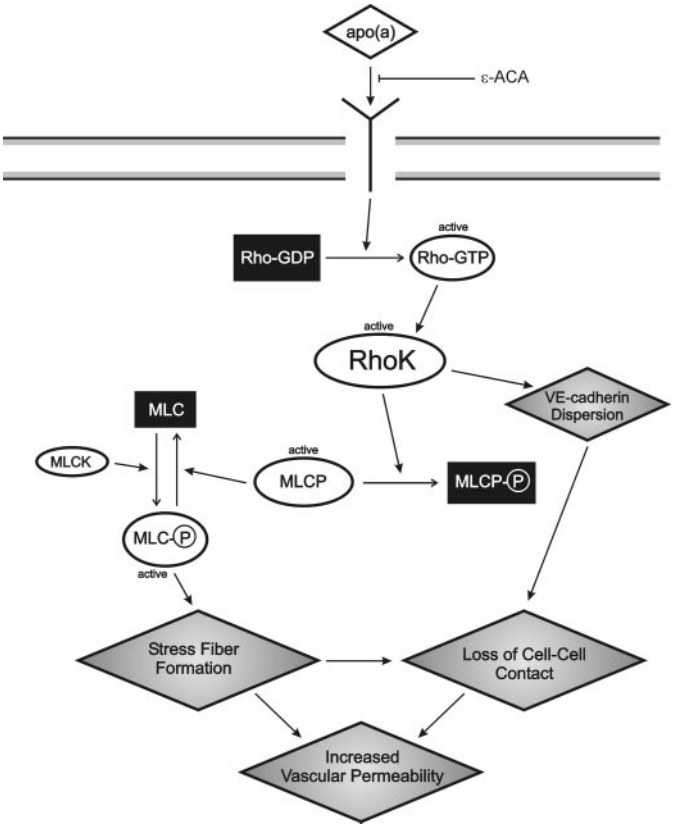

FIGURE 8. **Proposed model demonstrating signaling events involved in apo(a)-mediated endothelial cell contraction and increased permeability.** Binding of apo(a) to a putative receptor results in activation of Rho, which binds to and activates its downstream effector Rho kinase (*RhoK*). MLC is activated through phosphorylation of the MLC by Ca^{2+}/calmodulin-activated MLC kinase (*MLCK*). RhoK enhances MLC phosphorylation through inactivation of MLC phosphatase by direct phosphorylation of its 130-kDa regulatory subunit (MYPT1). RhoK is also able to promote VE-cadherin dispersion. This, together with increased stress fiber formation, combines to promote loss of cell-cell contact and thus decreased endothelial barrier function (*i.e.* increased vascular permeability). The effects of apo(a) are blocked by the lysine analogue ε-ACA.

binds to an as-yet identified receptor, which leads to increased MLC phosphorylation, stress fiber formation, and EC contraction in a Rho/RhoK/MYPT1-dependent pathway and where the activity of MLCK is not disrupted. Concomitantly, apo(a) induces a dispersion of VE-cadherin, which is the likely cause of the increased endothelial permeability elicited by apo(a). The VE-cadherin dispersion would be promoted mechanically by contraction of the actin cytoskeleton. In addition, apo(a) may promote the disassembly of adherens junctions through modulation of intracellular signaling pathways. In this regard, our preliminary data show that 17K mediates the dissociation of α- and γ-catenins from VE-cadherin complex while β-catenin translocates into the nucleus (data not shown). Our identification of KIV$_{10}$ as the domain in apo(a) that mediates cytoskeletal reorganization in endothelial cells may provide a novel therapeutic target for the early stages of atherosclerosis.

REFERENCES

1. Koschinsky, M. L. (2006) *Cardiovasc. Hematol. Disord. Drug Targets* **6,** 267–278
2. Anuurad, E., Boffa, M. B., Koschinsky, M. L., and Berglund, L. (2006) *Clin. Lab. Med.* **26,** 751–772
3. Koschinsky, M. L., Côté, G. P., Gabel, B., and van der Hoek, Y. Y. (1993) *J. Biol. Chem.* **268,** 19819–19825
4. McLean, J. W., Tomlinson, J. E., Kuang, W., Eaton, D. L., Chen, E., Fless, G., Scanu, A., and Lawn, R. M. (1987) *Nature* **330,** 132–137
5. Gabel, B. R., and Koschinsky, M. L. (1995) *Biochemistry* **34,** 15777–15784
6. van der Hoek, Y. Y., Wittekoek, M. E., Beisiegel, U., Kastelein, J. J. P., and Koschinsky, M. L. (1993) *Hum. Mol. Genet.* **2,** 361–366
7. Lackner, D., Cohen, J. C., and Hobbs, H. H. (1993) *Hum. Mol. Genet.* **2,** 933–940
8. Becker, L., McLeod, R. S., Marcovina, S. M., Yao, Z., and Koschinsky, M. L. (2001) *J. Biol. Chem.* **276,** 36155–36162
9. Sangrar, W., and Koschinsky, M. L. (2000) *Biochem. Cell Biol.* **78,** 519–525
10. Hughes, S. D., Lou, X. J., Ighani, S., Verstuyft, J., Grainger, D. J., Lawn, R. M., and Rubin, E. M. (1997) *J. Clin. Invest.* **100,** 1493–1500
11. Michel, C. C., and Curry, F. E. (1999) *Physiol. Rev.* **79,** 703–761
12. Schnittler, H. J., Wilke, A., Gress, T., Suttorp, N., and Drenckhahn, D. (1990) *J. Physiol.* **431,** 379–401
13. Goeckeler, Z. M., and Wysolmerski, R. B. (1995) *J. Cell Biol.* **130,** 613–627
14. Bodmer, J. E., Van Engelenhoven, J., Reyes, G., Blackwell, K., Kamath, A., Shasby, D. M., and Moy, A. B. (1997) *Microvasc. Res.* **53,** 261–271
15. Gündüz, D., Hirche, F., Härtel, F. V., Rodewald, C. W., Schäfer, M., Pfitzer, G., Piper, H. M., and Noll, T. (2003) *Cardiovasc. Res.* **59,** 470–478
16. Wojciak-Stothard, B., Entwistle, A., Garg, R., and Ridley, A. J. (1998) *J. Cell. Physiol.* **176,** 150–165
17. Lum, H., Ashner, J. L., Phillips, P. G., Fletcher, P. W., and Malik, A. B. (1992) *Am. J. Physiol.* **263,** L219–L225
18. Essler, M., Retzer, M., Bauer, M., Heemsker, J. W., Aepfelbacher, M., and Seiss, W. (1999) *J. Biol. Chem.* **274,** 30361–30364
19. Pellegrino, M., Furmaniak-Kazmierczak, E., LeBlanc, J. C., Cho, T., Cao, K., Marcovina, S. M., Boffa, M. B., Côté, G. P., and Koschinsky, M. L. (2004) *J. Biol. Chem.* **279,** 6526–6533
20. Garcia, J. G. N., Davis, H. W., and Patterson, C. E. (1995) *J. Cell. Physiol.* **163,** 510–522
21. Van Nieuw Amerongen, G. P., Draijer, R., Vermeer, M. A., and van Hinsbergh, V. W. M. (1998) *Circ. Res.* **83,** 1115–1123
22. Somlyo, A. P., and Somlyo, A. V. (2000) *J. Physiol.* **522,** 177–185
23. Kimura, K., Ito, M., Amano, M., Chihara, K., Fukata, Y., Nakafuku, M., Yamamori, B., Feng, J., Nakano, T., Okawa, K., Iwamatsu, A., and Kaibuchi, K. (1996) *Science* **273,** 245–248
24. Essler, M., Amano, M., Kruse, H. J., Kaibuchi, K., Weber, P. C., and Aepfelbacher, M. (1998) *J. Biol. Chem.* **273,** 21867–21874
25. Koschinsky, M. L., Tomlinson, J. E., Zioncheck, T. F., Schwartz, K., Eaton,

D. L., and Lawn, R. M. (1991) *Biochemistry* **30,** 5044–5051
26. Sangrar, W., Gabel, B. R., Boffa, M. B., Walker, J. B., Hancock, M. A., Marcovina, S. M., Horrevoets, A. J. G., Nesheim, M. E., and Koschinsky, M. L. (1997) *Biochemistry* **36,** 10353–10363
27. Becker, L., Cook, P. M., and Koschinsky, M. L. (2004) *Biochemistry* **43,** 9978–9988
28. Kawano, Y., Fukata, Y., Oshiro, N., Amano, M., Nakamura, T., Ito, M., Matsumura, F., Inagaki, M., and Kaibuchi, K. (1999) *J. Cell Biol.* **147,** 1023–1038
29. Marcovina, S. M., Koschinsky, M. L., Albers, J. J., and Skarlatos, S. (2003) *Clin. Chem.* **49,** 1785–1796
30. Angelin, B. (1997) *Curr. Opin. Lipidol.* **8,** 337–341
31. Boonmark, N. W., Lou, X. J., Yang, Z. J., Schwartz, K., Zhang, J. L., Rubin, E. M., and Lawn, R. M. (1997) *J. Clin. Invest.* **100,** 558–564
32. Allen, S., Khan, S., Tam, S., Koschinsky, M. L., Taylor, P., and Yacoub, M. (1998) *FASEB J.* **12,** 1765–1766
33. Takami, S., Yamashita, S., Kihara, S., Ishigami, M., Takemura, K., Kume, N., Kita, T., and Matsuzawa, Y. (1998) *Circulation* **97,** 721–728
34. Zhao, S. P., and Xu, D. Y. (2000) *Thromb. Res.* **100,** 501–510
35. Haque, N. S., Zhang, X., French, D. L., Li, J., Poon, M., Fallon, J. T., Gabel, B. R., Taubman, M. B., Koschinsky, M. L., and Harpel, P. C. (2000) *Circulation* **102,** 786–792
36. Sorensen, K. E., Celermajer, D. S., Georgakopoulos, D., Hatcher, G., Betteridge, D. J., and Deanfield, J. E. (1994) *J. Clin. Invest.* **93,** 50–55
37. Tsurumi, Y., Nagashima, H., Ichikawa, K., Sumiyoshi, T., and Hosoda, S. (1995) *J. Am. Coll. Cardiol.* **26,** 1242–1250
38. Schachinger, V., Halle, M., Minners, J., Berg, A., and Zeiher, A. M. (1997) *J. Am. Coll. Cardiol.* **30,** 927–934
39. Hancock, M. A., Boffa, M. B., Marcovina, S. M., Nesheim, M. E., and Koschinsky, M. L. (2003) *J. Biol. Chem.* **278,** 23260–23269
40. Belczewski, A. R., Ho, J., Taylor, F. B., Jr., Boffa, M. B., Jia, Z., and Koschinsky, M. L. (2005) *Biochemistry* **44,** 555–564
41. Redlitz, A., and Plow, E. F. (1995) *Baillieres Clin. Haematol.* **8,** 313–327
42. Kwon, M., MacLeod, T. J., Zhang, Y., and Waisman, D. M. (2005) *Front. Biosci.* **10,** 300–325
43. Babbin, B. A., Parkos, C. A., Mandell, K. J., Winfree, L. M., Laur, O., Ivanov, A. I., and Nusrat, A. (2007) *Am. J. Pathol.* **170,** 951–966
44. Guan, J. L. (2004) *Science* **303,** 773–774
45. del Pozo, M. A., Alderson, N. B., Kiosses, W. B., Chiang, H. H., Anderson, R. G., and Schwartz, M. A. (2004) *Science* **303,** 839–842
46. Palazzo, A. F., Eng, C. H., Schlaepfer, D. D., Marcantonio, E. E., and Gundersen, G. G. (2004) *Science* **303,** 836–839